Table 3 (*cont.*)

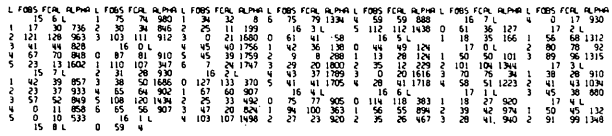

at the 0·005 significance level for a one-dimensional hypothesis and 2081 degrees of freedom.

Results

The final structure of $RbTh_3F_{13}$ is illustrated in Fig. 1. The two Th ions in the asymmetrical unit have nine nearest neighbor F ions at the corners of a trigonal prism with each of the prism faces capped by an F ion. The Th–F distances in both polyhedra range from 2·32 to 2·48 Å (Table 2) with minor differences in the standard errors. The Th(1) polyhedra form columns parallel to $\mathbf{b}_0$ by sharing edges and the shared edge, F(1)–F(6), alternates successively parallel to $\mathbf{a}_0$ at $y=0·5$ and parallel to $\mathbf{c}_0$ at $y=0·0$. The columns of Th(1) polyhedra are connected by corner sharing, F(2). The columns are intersected by layers of Rb ions and Th(2) polyhedra at $y=0·5$ and $y=0·0$ respectively. The layers are parallel to (010). Each Th(2) polyhedron shares an edge, F(3)–F(8), with each of two Th(1) polyhedra and a corner, F(4) and F(5), with each of four other Th(1) polyhedra. The F(1)–F(6) and F(3)–F(8) interatomic distances representing the shared edges are 2·50 (3) and 2·54 (2) Å respectively (Table 2). The Th(2) polyhedra do not touch one another. The Rb ions have eleven nearest neighbor F ions at distances of 2·79 (3) to 3·37 (2) Å.

References

BROWN, G. M. & LEVY, H. A. (1964). *J. Phys.* **25**, 597.

BUSING, W. R., MARTIN, K. O. & LEVY, H. A. (1962). *ORFLS. A Fortran Crystallographic Least-Squares Program.* ORNL-TM-305. Oak Ridge National Laboratory, Oak Ridge, Tennessee.

CROMER, D. T. & WABER, J. T. (1965). *Acta Cryst.* **18**, 104.

CROMER, D. T. (1965). *Acta Cryst.* **18**, 17.

HAMILTON, W. C. (1965). *Acta Cryst.* **18**, 502.

ZACHARIASEN, W. H. (1967). *Acta Cryst.* **23**, 558.

ZACHARIASEN, W. H. (1968). *Acta Cryst.* A**24**, 212.

Acta Cryst. (1971). B**27**, 1826

Refinement of the Structure of Sodium β-Alumina

BY C. R. PETERS AND M. BETTMAN

Scientific Laboratory, Ford Motor Company, Dearborn, Michigan, U.S.A.

AND J. W. MOORE AND M. D. GLICK

Department of Chemistry, Wayne State University, Detroit, Michigan, U.S.A.

(*Received* 15 *September* 1970)

An X-ray diffractometer re-investigation has been carried out on a clear crystal of fusion-cast sodium β-alumina, hexagonal, space group $6_3/mmc$, $a=5·594$, $c=22·53$ Å, $D_x=D_m=3·24\pm0·02$ g.cm^{-3}; probable unit-cell content = $Na_{2·58}\ Al_{21·81}\ O_{34}$. Using Mo $K\alpha$ radiation, 1175 measured intensities were combined into 545 symmetry-independent values of significant magnitude above background. A least-squares refinement based on these 545 data yielded $R_1=0·034$. The crystal was apparently typical in that both neutron activation analysis and X-ray intensity analysis found 29 % excess soda, relative to the classical formula Na_2O . 11 Al_2O_3. In the averaged unit cell, sodium atoms are smeared out in a complex pattern in the basal mirror plane. About 0·75 sodium atoms are near each of two Beevers–Ross positions, but spread into a broad triangular pattern. The remaining sodium scattering matter is in elongated ellipsoids centered near the positions that are halfway between the oxygen atoms of the basal mirror planes. This is a sixfold set of positions, containing a total of about one sodium ion. Indications are that the counter-ion defects consist of aluminum vacancies distributed over the (single) 12-fold set of aluminum atoms. Speculations are offered concerning the structure of local defects that would average out to the mean unit cell found.

Introduction

The main features of the β-alumina structure were deduced by Bragg, Gottfried & West (1931). These authors were troubled by the small percentage of sodium found by chemical analysis, which was inconsistent with the space-group symmetry and suggested a degree of randomness in the structure. Subse-

quently, improvements in the chemical analysis for sodium have led to higher and higher sodium percentages. Beevers & Ross (1937) redetermined the structure and arrived at the formula $Na_2O \cdot 11Al_2O_3$, with precisely described ordered positions for sodium and all the other atoms. This formula seemed to agree reasonably well with the analyses then available. We shall refer to it as the 'ideal formula'. The idealized structure is shown in Fig. 1 and is briefly described in the discussion section. More recent work, described below, suggests strongly that normal β-alumina crystals contain an excess of about 15 to 30% soda, relative to the ideal formula, and that we are dealing with an off-stoichiometric, massively defective structure. The present paper is an attempt to elucidate the nature of these defects.

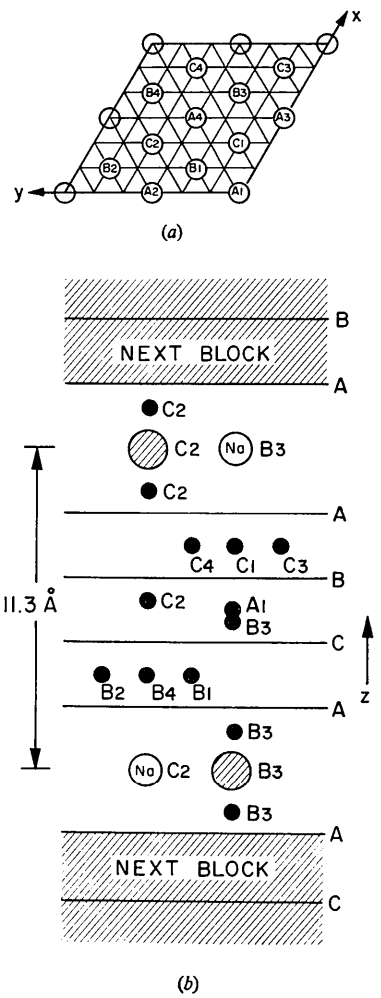

Fig. 1. Idealized Beevers–Ross structure. (*a*) Key to the *x*-*y* positions of β-alumina, showing one unit-cell cross section. To be used with Fig. 1(*b*). Letters *A*, *B*, and *C* have their usual close-packing connotation, but subscripts 1 to 4 are necessary because the *a*, *b* axes are doubled relative to the simplest kind of closepacked structure. Grid lines are drawn at intervals of *a*/6 and *b*/6, because the idealized *x*-*y* positions of all atoms are of the form *m*/6, *n*/6, with integral *m* and *n*. (*b*) Schematic projection of β-alumina onto the *b*-*c* plane. Aluminum atoms are small, solid circles whose *x*-*y* position is labeled according to the key of Fig. 1(*a*). Horizontal lines marked *A*, *B*, or *C* denote close-packed oxygen layers, in which all four positions of type *A*, or *B*, or *C* [see Fig. 1(*a*)] are occupied. The 'spacer-column' oxygen atoms are large, shaded circles. Sodium atoms are open circles, labeled Na.

J. Felsche (1968) published an X-ray redetermination of the β-alumina structure. He found the sodium sites suggested by Beevers & Ross to be only $\frac{1}{3}$ occupied, suggesting a sodium concentration far lower than even that of the ideal formula. Felsche obtained his crystal from 'the centre of a corroded, fusion-cast β-alumina refractory block which had been used for about two years as superstructure material in a tank for sheet glass'. It is our belief that Feslche worked on a highly atypical, leached-out crystal, and that 'typical' specimens are those produced under conditions of near equilibrium with adjacent phases in the Na_2O–Al_2O_3 system, and not subsequently reacted with other chemicals.

Interest in β-alumina has been revived in recent years by the discovery of its high sodium ion mobility by Kummer & Weber (1968). The ions can diffuse two-dimensionally in the basal mirror plane in which they are located. Typical resistivities are 30 ohm.cm at room temperature and about 1/10th of this at 300°C., when the electric field is parallel to the basal plane. Yao & Kummer (1967) discovered that many ions could be substituted for sodium in this structure by fused-salt ion exchange at moderate temperatures. They found that even the clearest crystals picked out of fusion-cast blocks had excesses of soda ranging from 15 to 30%. In recent phase-diagram work on the $NaAlO_2$–Al_2O_3 system, Weber & Venero (1969) investigated the composition range of the β phase to a limited degree. They found that at 1750°C the soda-to-alumina ratio ranges from 1:8·1 to 1:9·2, as opposed to the ratio of 1:11 in the idealized formula. Unless the β-phase field describes very unusual curvatures as a function of temperature, it appears that the ideal stoichiometric ratio of 1:11 is outside the equilibrium phase field at all temperatures.

It is true that wide variations from stoichiometry, both lean and rich in soda, have been reported in the literature for β-alumina. These wide variations are believed to be partly due to errors in the relatively difficult chemical analysis, and partly due to confusion with other similar phases, such as β''-alumina (Bettman & Peters, 1969) or '3-block-beta'. The reader is referred to a recent critical review by De Vries & Roth (1969), which, however, does not include the latest work by Weber & Venero (1969). Our point is that this most recent and painstaking work, coupled with the analyses of clear, fusion-cast crystals, indicates that the equilibrium phase field for binary β-alumina has a measurable, but quite limited width, all of it rich in soda relative to the idealized 1:11 formula.

In the present work we used a crystal that showed a typical excess of sodium both by neutron activation

analysis and in the analysis of the X-ray intensities. The actual distribution of sodium ions in the mirror plane of the averaged unit cell is somewhat complex and smeared out. It indicates a variation from unit cell to cell, both in the number of sodium atoms – necessitated by their nonintegral mean number – and in their positions. The latter variation is not unreasonable and is probably caused by the strong, distortionary electric fields of the counter-ion defects. There is a slight but statistically significant indication that these consist of aluminum ion vacancies distributed among a certain set of positions. Details are given in the discussion section.

Crystal data

The system is hexagonal, Laue symmetry 6/*mmm*. The only systematic absences are the *hhl*, $l=2n+1$. Our unit-cell constants were $a=5{\cdot}594$ and $c=22{\cdot}53$ Å. Following previous investigators, we assumed the space group D^4_{6h}, $P6_3/mmc$, No. 194. Previous density measurements (Beevers & Brohult, 1936) were in the range 3·23–3·26, which corresponds well to unit-cell contents in the vicinity of the idealized $Na_2O\,.\,11\,Al_2O_3$. Dr N. Weber measured the refractive indices of the crystal from which the X-ray specimen was cut. He found $n_E=1{\cdot}6254$ and $n_O=1{\cdot}6655$ for sodium *D* light.

Experimental

A clear crystal of approximate dimensions $2\times3\times0{\cdot}2$ mm was selected from a fusion-cast block of 'H-Brick' (Monofrax H, Harbison Carborundum Co., Falconer, N.Y.). An X-ray specimen of dimension $0{\cdot}18\times0{\cdot}18\times0{\cdot}36$ mm was cut from this crystal with a razor blade. The remaining major portion of the crystal was analyzed by neutron activitation analysis by Dr R. H. Marsh and Mr J. W. Butler (Marsh & Allie, 1968), who found $4{\cdot}93\pm0{\cdot}02\%$ by weight of sodium. This corresponds to 6·64% by weight of Na_2O, and to the formulas $Na_2O\,.\,8{\cdot}55\,Al_2O_3$ or $(Na_2O)_{1{\cdot}29}\,.\,11Al_2O_3$ or $Na_{2{\cdot}55}Al_{21{\cdot}82}O_{34}$. Intensities were collected on a Picker card controlled, four-circle diffractometer, using Mo $K\alpha$ radiation with a 2-mil Zr β-filter and the θ–2θ scan technique. Peaks were scanned at a rate of 2°/min with 10 sec stationary background counts at both ends of the scan. The crystal was offset so that no symmetry axis coincided with the φ axis of the instrument, thus reducing the probability of serious multiple diffraction problems. Data were collected for a 60° section of the $l\geq0$ hemisphere comprising two asymmetric units, out to $\sin\theta$ of 0·6. Two strong reflections were used as standards and were monitored at regular intervals. They showed a positive drift of 1% from the beginning to the end of the experiment.

The 1175 measured intensities were corrected for background, Lorentz–polarization factors, and absorption. The absorption program, provided by B. Wuensch, also computed the path-dependent secondary extinction variable β as defined by Zachariasen (1963).

Structure refinement

Least-squares program (Busing, Martin & Levy, 1962) *ORFLS* was modified to allow variation of the secondary extinction parameter *C* in Zachariasen's formula $F_o\simeq yF_c=kF_c/(1+\beta I_oC)$. The quantity $\sum w(F_o-yF_c)^2$ was minimized by the program. For the

Table 1. *Observed and calculated structure factors*

Values listed for F_o and F_c are in electron units × 10. For unobserved reflections, $F_o=0$.

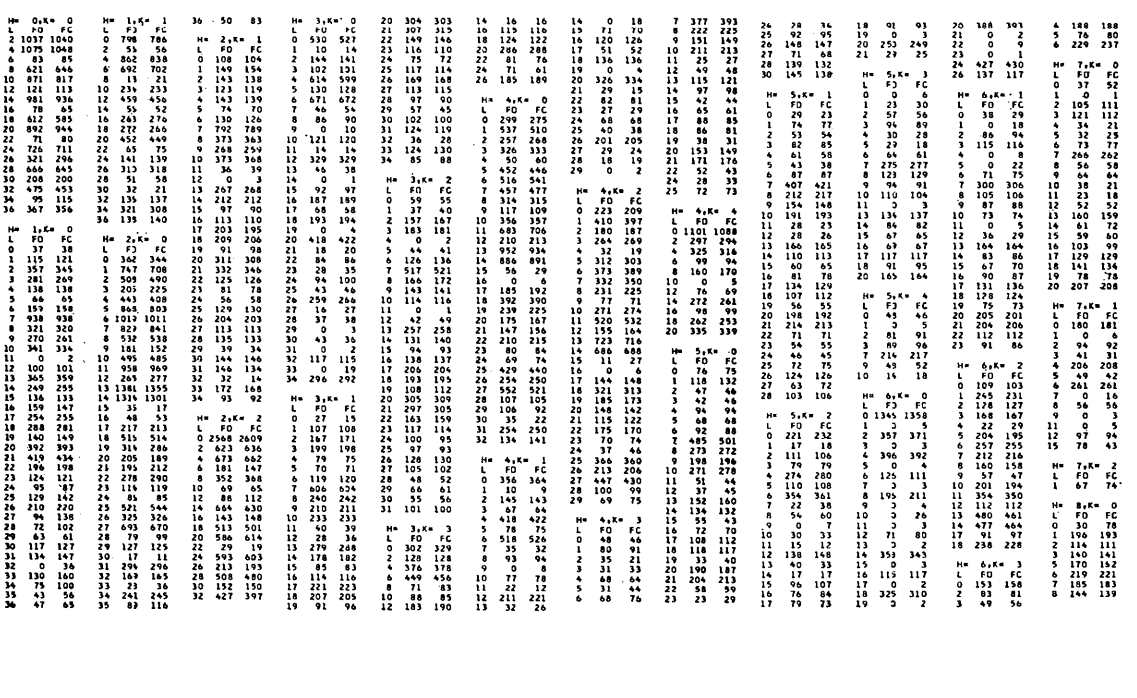

initial cycles of least-squares refinement, the weights w were taken as : $w=1/(n\sigma^2)$. Here n is the number of times a given reflection was measured and σ is the standard deviation based on the counting statistics of the integrated peak and the two background counts. The aim of the initial refinement was to determine a good value for the secondary extinction coefficient, C. The value for C turned out to be small, leading to a 7·5% correction of F_o in the worst case. The factor $1/y$ was then absorbed into each observed F, putting it on an absolute basis in electron units. It was now possible to average symmetry-equivalent reflections into one asymmetric unit, taking the weighted average of symmetry equivalents with the weights w described above. This resulted in 633 F values, of which 545 were above background by more than two standard deviations of the background. The 545 values were used for subsequent refinements. To each value we assigned a standard deviation $\sigma'(F)=[\bar{\sigma}^2+(pF_o)^2]^{1/2}$, where $\bar{\sigma}$ is equal to $\left[\sum\frac{1}{\sigma^2}\right]^{-\frac{1}{2}}$, summing over symmetry equivalents, and σ is the counting statistical value defined above. The factor pF_o amounts to assigning a percentage error to each F value to prevent overweighting strong intensities. The new weights, w', were set equal to the reciprocal square of σ'. We chose $p=0{\cdot}03$, which led to a final 'goodness of fit' $[\sum w'(F_o-F_c)^2/(n-m)]^{1/2}$, of 1·37. Observed and calculated structure factors are listed in Table 1.

Course of the refinement

For the four aluminum atoms and five oxygen atoms in the asymmetric unit, the coordinates determined by earlier workers were used as starting parameters, along with a reasonable set of anisotropic thermal parameters. Form factors for Na^{1+}, O^{1-}, and $Al^{1\cdot5+}$ (the latter two by interpolation) were taken from Cromer & Waber (1965) and Tokanami (1965). A sodium atom was fixed at the position $(\frac{2}{3},\frac{1}{3},\frac{1}{4})$ with full occupation. This is the Beevers–Ross (hereafter BR) position for sodium in the idealized structure. The excess 0·29 sodium (according to activation analysis) in the asymmetric unit was placed at $(0,0,\frac{1}{4})$, hereafter called the anti-Beevers–Ross (aBR) position. Beevers & Ross had considered these two as either/or alternatives for complete occupation and found that the BR alternative gave better agreement. During subsequent refinement the occupation of the BR decreased, the occupation for aBR increased, and both, but especially the aBR, developed unrealistically high temperature factors for in-plane displacements (*i.e.* β_{11}). A difference Fourier section and a Fourier section at $z=\frac{1}{4}$, the latter similar to the final one of Fig. 2, demonstrated the difficulty: scattering matter in the BR position, but it is broadly distributed about the position in a triangular pattern. On the other hand, there is almost nothing in the immediate vicinity of the aBR position. The excess sodium appears near $(\frac{5}{6},\frac{1}{6},\frac{1}{4})$ *etc.*, the midpoint between 'column oxygens'. This position is referred to as the mid-oxygen (mO) position. Fig. 2 suggests that the electron density near the mO position can be represented by the fusion of two lumps of density, one just about at the mO position, the other shifted by perhaps 0·5 Å to about (0·888, 0·112, $\frac{1}{4}$). In subsequent least-squares refinement we attempted to represent the density near mO by two fractional atoms, varying the occupation number, the X parameter, and three thermal parameters for each. This led to convergence problems because of severe correlations between some of these parameters. Therefore we limited ourselves to representing the density near the mO position by a single atom, varying x, the occupation number, and the three thermal parameters appropriate for the intersection of two mirror planes. The eccentricity of the thermal ellipsoid then tended to approximate the density distribution. The x parameter took the intermediate value of 0·8731. On the other hand, the triangular distribution around the BR position was handled in the least-squares program by splitting it into three atoms, each slightly offset from the threefold axis, and each given the more general three-parameter thermal ellipsoid, instead of the two-parameters one appropriate for the triad that goes through the BR position. The occupancy of the BR position was also varied, of course. This type of strategy for the least-squares program represents an attempt to approximate the somewhat smeared-out electron distribution at $z=\frac{1}{4}$, as indicated by the Fourier section of Fig. 2. The final difference Fourier section of Fig. 3 shows that these approximations are adequate. Its peaks and valleys range from +0·4 to −0·5 e.Å^{-3}, which is close to the expected error in these positions according to the criteria of Cruickshank

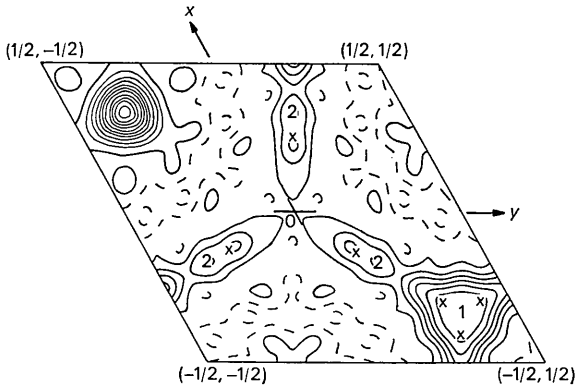

Fig. 2. Fourier section showing electron density of β-alumina in mirror plane at $z=\frac{1}{4}$. Sites marked X show the placement by least-squares of fractional, thermally anisotropic Na atoms, see Table 2, which approximate the electron distribution near sites 1 and 2. These are the Beevers–Ross and mid-oxygen sites, respectively at $(-\frac{1}{3},\frac{1}{3},\frac{1}{4})$ and $(-\frac{1}{6},\frac{1}{6},\frac{1}{4})$. Note that there is virtually no electron density at $(0,0,\frac{1}{4})$, the anti-Beevers–Ross site. Initial solid contour drawn at 1 e.Å^{-3}, with an interval of +1 e.Å^{-3} for regions 1 and 2, and an interval of +1·5 for the oxygen atom, O(5), centered at $(\frac{1}{3},-\frac{1}{3},\frac{1}{4})$. Dashed contours drawn using an interval of −1 e.Å^{-3} starting at 0 e.Å^{-3}.

& Rollett (1953). Both Fourier and difference Fourier sections give some indications of a triangular distribution for the oxygen atom at $\frac{1}{3},\frac{2}{3},\frac{1}{4}$. One can get convergence of the least-squares refinement after splitting this oxygen off-axis, but the improvement in R_2 is not significant according to Hamilton's statistical criteria (1965). At this point, $R_1=[\sum||F_o|-|F_c||]/\sum|F_o|$ was 0·035 and $R_2=[\sum w(F_o-F_c)^2/\sum wF_o^2]^{1/2}$ was 0·0533, and 46 parameters had been independently adjusted by least-squares methods. For each unit cell, $1{\cdot}5_0$ sodium atoms were near the BR positions and $1{\cdot}0_4$ were near the mO positions.

Search for counter-ion defects

To maintain electrical neutrality there must be negative countercharges to the excess positive sodium ions. Various considerations of physical properties make it unlikely that the countercharges consist of electrons or reduced sodium or reduced aluminum (see discussion). The most likely countercharges are either extra oxygen atoms in the basal mirror planes, or aluminum vacancies. Some of the extra scattering matter found in the mirror planes could, indeed, be due to extra oxygen. However, when analyzed as being sodium exclusively, it leads to nearly the same percentage of excess sodium, 27%, *vs.* the 29% found by activation analysis. In order to obtain possible indications of aluminum vacancies, we introduced eight more parameters, varying the occupation number of all sets of atoms, while necessarily keeping the scale factor fixed. This yielded $R_1=$ 0·0337, $R_2=0{\cdot}0499$. A total of 54 parameters had now been varied for the adjustment of 545 observations. (53 of these parameters were actually varied during the final cycles of least-squares refinement, the 54th being the extinction constant, frozen at an earlier stage.) The improvement in R_2 as a result of the 8 additional occupation parameters is significant on the 0·995 confidence level, according to Hamilton's tables. The results of the occupancy variation are given in column 4 of Table 2, under the heading 'occupancy correction factor'. The total number, per unit cell, in a given set of atoms is obtained by multiplying this factor by the multiplicity of the set, given in column 2 of Table 2.

All oxygen occupation correction factors equal each other to within their standard deviations. On physical grounds, we expect either excess interstitial oxygen or aluminum vacancies, but not oxygen vacancies. Therefore a normalization factor was applied to all occupation correction factors (column 4 of Table 2) so as to make them unity, on the average, for the oxygen atoms.

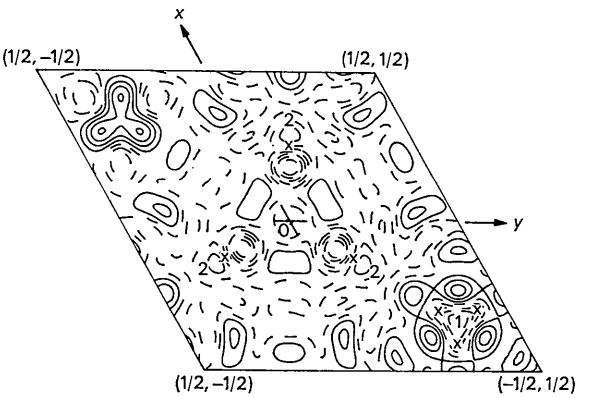

Fig. 3. Difference Fourier section of β-alumina in mirror plane at $z=\frac{1}{4}$, showing residual errors resulting from model assumed for the electron distribution in this plane. Labeling is the same as in Fig. 2. Solid contours drawn using an interval of 0·1 e.Å^{-3} starting at 0 e.Å^{-3}, and dashed contours, using an interval of $-0{\cdot}1$ e.Å^{-3} starting at 0 e.Å^{-3}.

Table 2. *Positional,* thermal,† and occupation parameters for β-alumina*

	No. of equipoints, Wyckoff notation	Site symmetry	Occupancy correction factor‡	*X*	*Z*	β_{11}	β_{33}	β_{12}	β_{13}
O(1)	12 (*k*)	*m*	0·996 (9)	0·15711 (12)	0·05011 (6)	51 (4)	2·3 (2)	37 (4)	0·1 (4)
O(2)	12 (*k*)	*m*	0·998 (9)	0·50318 (14)	0·14678 (6)	38 (4)	3·4 (2)	16 (4)	0·2 (4)
O(3)	4 (*f*)	3*m*	0·993 (12)	$\frac{2}{3}$	0·05552 (10)	53 (6)	1·1 (3)	$\beta_{11}/2$	0
O(4)	4 (*e*)	3*m*	1·014 (11)	0	0·14253 (9)	45 (5)	2·2 (3)	$\beta_{11}/2$	0
O(5)	2 (*c*)	$\bar{6}$*m*2	1·018 (21)	$\frac{1}{3}$	$\frac{1}{4}$	548 (27)	2·3 (7)	$\beta_{11}/2$	0
Al(1)	12 (*k*)	*m*	0·989 (6)	−0·16775 (6)	0·10630 (3)	49 (2)	2·6 (1)	28 (2)	0·1 (2)
Al(2)	4 (*f*)	3*m*	1·028 (8)	$\frac{1}{3}$	0·02477 (4)	38 (3)	2·3 (2)	$\beta_{11}/2$	0
Al(3)	4 (*f*)	3*m*	1·006 (8)	$\frac{1}{3}$	0·17555 (4)	53 (3)	1·5 (2)	$\beta_{11}/2$	0
Al(4)	2 (*a*)	$\bar{3}$*m*	1·025 (10)	0	0	39 (4)	2·4 (2)	$\beta_{11}/2$	0
Na(1)§	6 (*h*)	*mm*	0·250 (12)	−0·2938 (21)	$\frac{1}{4}$	668 (99)	12 (1)	147 (78)	0
Na(2)	6 (*h*)	*mm*	0·174 (15)	−0·1269 (63)	$\frac{1}{4}$	858 (118)	12 (3)	−396 (130)	0

* For all atoms $y=-x$; estimated errors, (in parentheses), of right-most digits, calculated from variance-covariance matrix of least-squares program.

† Temperature factor of form: $\exp-[(h^2+k^2)\beta_{11}+l^2\beta_{33}+2hk\beta_{12}+(2hl-2kl)\beta_{13}]\times 10^{-4}$

‡ Number of equipoints × occ. factor = number of atoms per unit cell.

§ These are really the 2(*d*) BR Na sites. Each site has been tripled with the 6(*h*) positions only slightly removed from the triad axis. Because of overlap, only one member of a given triplet may be occupied. Thus, the maximum occupancy of these sites is 2/unit cell. Actually, $6\times 0{\cdot}250=1{\cdot}50$ Na atoms/unit cell are observed.

Chemical analysis, combined with experimental density, supports this but only to within an uncertainty of about one per cent. Note that there is no deficiency in the 'column oxygen', O(5), such as seen by Felsche (1968).

On the other hand, the variation in the occupancy factors for the aluminum atoms seems well outside the range of statistical errors, judging by their standard deviations. Particularly, the occupancy of the 12-fold set Al(1), Table 2, is five standard deviations below the number-weighted average occupation number for the remaining aluminum atoms, *i.e.* about 1·019*. The fourfold set, Al(3), is also somewhat low.

Discussion

Aluminum–oxygen distances in β-alumina are shown in Table 3. The idealized structure proposed by Beevers & Ross is shown in Fig. 1. It consists of two 'spinel blocks', related to each other by the two basal mirror planes at $z=\frac{1}{4}$ and $z=\frac{3}{4}$. Each block consists of four layers of cubic-close-packed oxygen ions. Three aluminum atoms are sandwiched between each pair of oxygen layers, giving the typical M_3O_4 alternation of spinel. The aluminum atoms are in both octahedral and tetrahedral interstices of the oxygen ions. They assume the same set of positions as the combined sets of positions of magnesium and aluminum in $MgAl_2O_4$ spinel. Across the basal mirror planes the two spinel blocks are joined by an Al–O–Al column. This linkage can alternatively be described as two AlO_4 tetrahedra with a common oxygen vertex in the mirror plane, the two sets of three basal oxygen atoms being part of each spinel block. Beevers & Ross were looking for a perfect structure and believed they had two Na atoms per unit cell. They had two sets of twofold positions left over from the aluminum–oxygen network: one set at $(\frac{2}{3},\frac{1}{3},\frac{1}{4})$, *etc*, and the other set at $(0,0,\frac{1}{4})$, *etc*. They felt that they obtained a distinctly better comparison of calculated *vs.* observed intensities for the first mentioned set. We have referred to the first set as the BR position, and to the second set as the aBR position. The BR position is in the center of a trigonal prism of nearest neighbor oxygen atoms, about 2·88 Å away. These are part of the nearest layers of close-packed oxygen ions of the spinel blocks above and below the mirror plane. In addition, there are three next-nearest oxygen neighbors, at a distance of 3·23 Å, consisting of the 'column' oxygen atoms, in the same basal mirror plane. The aBR position has two nearest neighbor oxygen atoms directly above and below, at a distance of 2·39 Å, and the same three lateral next-nearest neighbors of column oxygen atoms.

Table 3. *Aluminum–oxygen distances* in β-alumina*

(*a*) Octahedra	Multiplicity	Distance (Å)
Al(1)–O(1)	2	2·022
–O(3)	1	1·970
–O(2)	2	1·837
–O(4)	1	1·819
Al(4)–O(1)	6	1·895
(*b*) Tetrahedra		
Al(3)–O(2)	3	1·768
–O(5)	1	1·677
Al(2)–O(1)	3	1·801
–O(3)	1	1·809

* Standard deviations in distances are 0·002 Å, based on least-squares standard deviations in coordinates.

Even on the basis of the ideal BR structure, one would expect considerable sodium ion mobility for two reasons: (1) The mirror plane is only about 50% full, containing an oxygen atom and a sodium atom in an area large enough for four oxygen atoms (*e.g.* in the blocks). There is so much vacant space that one need not invoke a vacancy mechanism and be limited by the vacancy concentration. (2) The Al–O–Al 'spacer column' keeps the two spinel blocks apart. The result is that one can trace out long range paths for the sodium ion such that the distance from any point on the path to the nearest oxygen ion is larger than or equal to, but never smaller than, the sum of the sodium (0·96–1·00 Å) and oxygen (1·40 Å) ionic radii. Nevertheless, it seems reasonable that the off-stoichiometric excess of sodium affects the transport of sodium ions profoundly. Yao & Kummer (1967) assumed the excess sodium ions to be in the aBR position, which they considered to be the interstitial position, and suggested an interstitialcy mechanism of diffusion. They also cited some evidence for decreasing sodium ion conductivity with decreasing sodium ion concentration.

We find the sodium distribution to be considerably more complex. In the first place, the BR position is only about 75% occupied. Secondly, the distribution of electron density around this site is very broad and triangular, as the Fourier section of Fig. 2 clearly shows, In our least-squares refinement we consider this distribution as the superposition of three split atoms, each removed from the BR position by 0·39 Å, and each having a three-parameter thermal ellipsoid. The distribution around the BR position could be explained in two ways: (1) a large amplitude thermal motion, (2) random distortions away from the BR position. We are inclined toward the latter view, and think the distortions are produced by the electric fields from the counter-ion defects, discussed below. Repetition of this work at low temperatures would presum-

* The fact that this number is slightly greater than unity is not considered significant. It is sensitive to the relative accuracy of the tabulated form factors for oxygen and aluminum. The main thrust of our argument depends on comparing only the aluminum occupation factors among themselves. This reasoning is tacitly based on the less severe assumption that all aluminum atoms in the structure are equally good X-ray scatterers.

ably settle the question. Fig. 2 shows that there is practically no electron density at the aBR position, in contrast to the quite natural supposition by Yao & Kummer; however, there exists another reasonable position for positive ions in the basal mirror plane. This is halfway between the 'column oxygens' at $(\frac{5}{6},\frac{1}{6},\frac{1}{4})$, *etc.* This third position is also in the center of a trigonal pyramid of oxygen atoms above and below. The mid-oxygen (mO) position is sixfold, and therefore was not considered by Beevers & Ross who were looking only at twofold positions. Fig. 2 shows that the remaining scattering matter is near this set of positions, in a somewhat elongated and distorted fashion. By least-squares methods we find 1·06 atoms near the mO positions [Na(2) in Table 2], and 1·51 atoms near the BR positions [Na(1) in Table 2]. Thus we find a total of 2·57 sodium ions per unit cell instead of the ideal two. The neutron activation analysis result corresponds to 2·58 sodium ions per unit cell. Such an occupation number, determined from X-ray intensities, does not have a high precision, so that the excellent agreement is somewhat fortuitous. Incidentally, the reader should note that in ion-exchanged β-alumina, other ions do not necessarily assume the same positions as the sodium ions. It is known that in silver-beta the excess silver ions are in the vicinity of the aBR positions (Roth, 1970).

The excess sodium ion concentration necessitates some kind of countercharge. Conceivably, this could consist of electrons, but we consider this possibility extremely unlikely. It would mean that either the sodium or aluminum exist in a somewhat reduced condition. Neither of these elements has such a tendency, especially when the compound in question is crystallized in air, as in the case of β-alumina. Further, one would then expect a deeply colored, mixed-valence crystal instead of the actually colorless crystals. All workers who treat the β-alumina formula as $Na_2O\,.\,x\,Al_2O_3$ or $(Na_2O)_{1+\varepsilon}.11Al_2O_3$ are already making the tacit assumption of complete oxidation of sodium and aluminum. It is far more likely, then, that the counter defects are ionic. The simplest candidates are (1) excess oxygen ions in the basal mirror plane (for which there is room) or (2) aluminum vacancies. We cannot rule out (1) because some of the excess scattering matter in the basal mirror plane could be oxygen instead of sodium. On the other hand, we have some definite evidence of (2). The occupancy of the 12-fold aluminum atoms, Al(1) of Table 2, is 3 ± 1% below the mean occupancy of the remaining aluminum atoms. The deficit is definitely statistically significant (see refinement section). Of course, one cannot rule out the possibility that systematic errors may account for this result. It could, for instance, be partly due to variations in the electron density distribution around, and hence the scattering power of, the various aluminum atoms. The amount of the deficit is approximately correct but somewhat high: multiplied by 3 for the triple charge on an Al vacancy and by 12 for the number of aluminum atoms in this set per unit cell; the deficit can account for $(0{\cdot}030\pm0{\cdot}010)(3)(12)=1{\cdot}1\pm0{\cdot}4$ excess sodium atoms per cell, whereas we only find about 0·54. These aluminum positions are directly above and below the mO position where we find the excess sodium.

One might, perhaps, have expected the aluminium vacancies to occur in the fourfold aluminum positions of the 'spacer column' aluminum atoms, Al(3) of Table 2. These are closest to the mirror plane, whereas the previously discussed 12-fold set is the next-nearest set. The occupation number of the Al(3) set is, indeed, somewhat low. However, if the aluminum vacancies were exclusively in this fourfold set, it should show a deficit occupancy of about 5%, relative to the other aluminum atoms, including Al(1), and we should have seen this.

There is an unlimited number of alternate, but more complex and farfetched, possibilities for the counter-ion defects. For instance, one might imagine that a few of the Al–O–Al columns are missing. Each missing column would account for four excess sodium atoms. Again, however, if these were the only defects, we would expect a 7% deficiency in the column aluminum and oxygen atoms, relative to the remaining aluminum and oxygen atoms, respectively. This is clearly not the case.

The fact that the BR position for sodium shows only about 75% occupancy is interesting. We would like to advance two possible explanations: (1) the sodium ions are undergoing a disordering at room temperature and the BR position is fully occupied at sufficiently low temperatures; (2) the strong local electric fields from the counter defects, presumably aluminum vacancies of effective charge -3 ,tend to completely dislodge the closest sodium ions in BR positions. Again, a low-temperature study would distinguish between these possibilities. We are inclined toward explanation (2) for three reasons: (*a*) Yao & Kummer (1967) found that the room temperature self-diffusion coefficient lies on the same semilog line as the higher temperature values; (*b*) Radzilowski, Yao, & Kummer (1969) found the same activation energy for the frequency of maximum loss *vs.* $1/T$ from dielectric loss measurements on sodium β-alumina near 100 °K; (*c*) we made differential thermal analysis measurements and could find no features in the room-temperature range. A disordering in the room-temperature range would be expected to change the transport properties and to exhibit a thermal effect, although our instruments may not have been sensitive enough for the latter.

It is to be emphasized that our X-ray analysis can only yield an averaged unit cell. One is tempted to speculate on the type of local defect structure that will produce this average. Let us for the moment accept all previously discussed indications, even those that are only weakly supported. The smallest defect cluster then must be $V_{Al}Na_3$, *i.e.* an aluminum vacancy associated with three excess sodium atoms in its vicinity. The oc-

cupation numbers found for the average unit cell can be well approximated if we assume that near each V_{Al} there are six sodium atoms in mO positions while three sodium atoms have been totally dislodged from BR positions. One could use the notation $V_{Al}[V_{Na(BR)}]_3\,[Na(mO)]_6$ for this hypothesis. The hypothesis seems reasonable for the following reason: the BR and mO positions are so close to each other that the sodium atom cannot locally coexist in both. In the vicinity of a V_{Al}, therefore, a small patch of BR positions are emptied in order to make available the more populous mO positions.

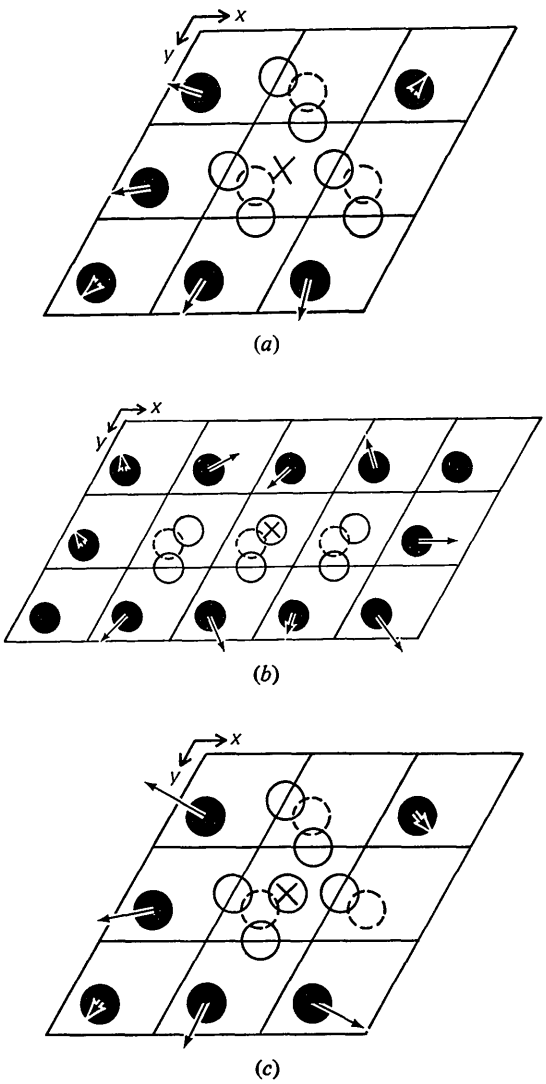

Fig. 4. Three models, (*a*), (*b*) and (*c*), for minimum size local defects. The unit-cell origin has been shifted so that the intersections of the hexagonal grid lines correspond to the positions of the basal mirror plane oxygen atoms, the 'column oxygens', which are not explicitly shown. Solid circles are filled BR positions. Solid-lined open circles are filled mO positions. Dotted circles are emptied BR positions. The aluminum vacancy, located 3·23 Å above or below the plane of the figure, is shown by an × mark. In each model the defect consists of an aluminum vacancy, three BR Na vacancies, and six mO Na interstitials. Direction and relative magnitude of the x,y components of the electric fields at peripheral BR sodium atoms is indicated by arrows.

Fig. 4 shows three variations of minimum-size clusters with the properties described above. There may be others that we missed, but we think the total number of sensible possibilities is not large. In Fig. 4, the origins have been shifted so that the intersections of the hexagonal grid lines correspond to the basal-plane oxygen atoms, O(5) of Table 2, which are not otherwise shown. Full black circles are BR sodium atoms, open dotted circles are missing BR sodium atoms, and open full circles are mO sodium atoms. The aluminum vacancy is indicated by a cross, but is located 3·23 Å above or below the plane of the figure. We have made some electrostatic calculations, described below, which slightly favor model (*a*) of the three models in Fig. 4. The arrows at the circumferential BR sodium atoms around each model are proportional in length and direction to the x,y projection of the electric field, due to the defect cluster, calculated at these points. It must be remembered from Fig. 2 that even those BR sodium atoms which are not totally dislodged are randomly distorted from the ideal BR position in a smeared-out triangular pattern. This presumably means that BR sodium atoms in the vicinity of a defect cluster are displaced in the direction of their local electric field. In this sense the arrows around model 4(*a*) in Fig. 4 agree better with the distribution in Fig. 2 than do the arrows of models (*b*) or (*c*).* Further, the electrostatic self-energy of defect (*a*) is somewhat lower that than of defect (*b*), which is lower than that of defect model (*c*).

Electrostatic calculations for defect models of Fig. 4(*a*), (*b*) and (*c*) are given in Table 4. The calculated electrostatic fields due to the neighboring defect are equal to $\mathbf{E}_i=\sum_j Q(j)\mathbf{r}_{ij}/|r_{ij}|^3$. The corresponding self-energy was taken to be $W=\sum_{i<j} Q(i)Q(j)/|r_{ij}|$. Two different calculations were made for each case. In the first, the charges $Q(j)$ were taken as -3 for the aluminum vacancy, -1 for each of the three missing BR sodium atoms, and 1 for each of the six mO sodium atoms. In the second calculation, the -3 charge of V_{Al} was devided into six negative half-charges and placed on the members of the oxygen octahedron surrounding it. The two calculations gave very similar results in all three cases.

It is, of course, possible that the defect clusters are dimerized or polymerized. In such a case the number

* For each model, its mirror image across the vertical mirror planes is equally likely to occur. For each two-mirror image, there are three equivalent rotational positions. The bases of all the arrows of all the symmetry equivalents of a model must be superposed at the BR position of the averaged cell, to decide which model is most likely to produce the observed electron density distribution around the BR position in the averaged cell.

of possibilities becomes very large. It could be, for example, that the clusters aggregate in patches of an incipient superstructure, interspersed with patches of ideal BR structure. Even if there is no purposeful aggregation, there will be some statistical polymer clusters because their concentration is rather high. The mean distance between separated clusters is only about 3·3 unit cells.

Table 4. *Electrostatic calculations for defect models of Fig.* 4(*a*), (*b*) *and* (*c*)

	Energy of defect* (eV)		Max. *xy* component† of electric field (10^7 volts/cm) at surrounding BR sites	
	Calculation method‡		Calculation method‡	
	1	2	1	2
Model				
4(*a*)	−56·91	−37·60	4·26	4·48
4(*b*)	−56·24	−36·49	5·90	6·01
4(*c*)	−55·45	−35·10	6·96	7·17

* The zero of energy of these numbers has no significance. Only the differences (of about 1 eV) between one model and another, within a given calculation method, are meaningful, *e.g.* the energies of method 2 are much higher than those of method 1 because of the repulsive self-energy of the six negative half-charges in the former.

† These values are proportional to the lengths of the longest arrows in Fig. 4(*a*), (*b*) and (*c*). Relative lengths of other arrows can be estimated from figures. Both methods of calculation always agree on which is the longest arrow.

‡ See text, next to last paragraph.

References

BEEVERS, C. A. & BROHULT, S. (1936). *Z. Kristallogr.* **95**, 472.

BEEVERS, C. A. & ROSS, M. A. (1937). *Z. Kristallogr.* **97**, 59.

BETTMAN, M. & PETERS, C. R. (1969). *J. Phys. Chem.* **73**, 1774.

BRAGG, W. L., GOTTFRIED, C. & WEST, J. (1931) *Z. Kristallogr.* **77**, 255.

BUSING, W. R., MARTIN, K. O. & LEVY, H. A. (1962). *ORFLS. A Fortran Crystallographic Least-Squares Program.* Report ORNL–3794. Oak Ridge National Laboratory, Oak Ridge, Tennesse.

CROMER, D. T. & WABER, J. T. (1965). *Acta Cryst.* **18**, 104.

CRUICKSHANK, D. W. J. & ROLLETT, J. S. (1953). *Acta Cryst.* **6**, 705.

DEVRIES, R. C. & ROTH, W. L. (1969). *J. Amer. Ceram. Soc.* **52**, 364.

FELSCHE, J. (1968). *Z. Kristallogr.* **127**, 94.

HAMILTON, W. C. (1965). *Acta Cryst.* **18**, 502.

KUMMER, J. T. & WEBER, N. (1968). *Trans. S. A. E.* **76**, 1003.

MARSH, R. H. & ALLIE, W., JR (1968). *Anal. Chem.* **40**, 2037.

RADZILOWSKI, R. H., YAO, Y. F., & KUMMER, J. T. (1969). *J. Appl. Phys.* **40**, 4716.

ROTH, W. L. (1970) Abstract No. I3, A. C. A. Summer Meeting (August) at Ottawa.

TOKANAMI, M. (1965). *Acta Cryst.* **19**, 486.

WEBER, N. & VENERO, A. F. (1969). Ford Motor Company Scientific Research Staff Technical Report No. SR69–86. To be published. Presented at the Amer. Ceram. Soc. Meeting, Philadelphia, May, 1970.

YAO, Y. F. & KUMMER, J. T. (1967). *J. Inorg. Nucl. Chem.* **29**, 2453.

ZACHARIASEN, W. H. (1963). *Acta Cryst.* **16**, 1139.